

IFUSP/P 440  
B.L.F. - USF

**UNIVERSIDADE DE SÃO PAULO**

**INSTITUTO DE FÍSICA  
CAIXA POSTAL 20516  
01498 - SÃO PAULO - SP  
BRASIL**

# publicações

IFUSP/P-440



PHOTOFISSION OF  $^{232}\text{Th}$

by

J.D.T. Arruda-Neto, W. Rigolon, S.B. Herdade,  
and H.L. Riette

Instituto de Física, Universidade de São Paulo

Novembro/1983

PHOTOFISSION OF  $^{232}\text{Th}^*$

J.D.T. Arruda-Neto, W. Rigolon, S.B. Herdade, and H.L. Riette

Instituto de Física, Universidade de São Paulo  
São Paulo, Brazil

ABSTRACT

The bremsstrahlung-induced fission cross section of  $^{232}\text{Th}$  was measured in the energy region of the Giant Dipole Resonance. The data analysis, performed in terms of the bremsstrahlung spectrum calculated in the Davies-Bethe-Maximon approximation, suggested that the photofission cross section measured at Livermore is correct, and that the  $(\gamma, f)$  data from Saclay are highly questionable.

Keyword abstract

NUCLEAR REACTION  $^{232}\text{Th}(\gamma, f)$ ,  $E = 20 - 32$  MeV, bremsstrahlung photon beam; measured  $\sigma(E)$ . Deduced the strength for the fission decay of the giant dipole resonance. Natural targets.

PACS: 24.30.Cz , 25.20.+y , 25.85.Jg , 27.90.+b

---

\*Supported in part by the Conselho Nacional de Desenvolvimento Científico e Tecnológico and by the Fundação de Amparo à Pesquisa do Estado de São Paulo.

The characteristics of the fission decay of the isoscalar Giant Quadrupole Resonance (GQR), namely, branching ratio and strength distribution for actinide nuclei, have been studied by means of hadron- and electron-induced reactions. The results from all these studies are controversial and somewhat obscure (Refs. 1 and 2, and references therein). The analysis of electron-induced reactions [inclusive electrofission (e,f) and coincident electrofission (e,e'f)] requires the knowledge of precise photofission cross sections  $\sigma_{\gamma,f}$ . For the (e,f) data analysis the  $\sigma_{\gamma,f}$  are used in the subtraction of the Giant Dipole Resonance (GDR) contribution to the total electrofission yield<sup>1,2)</sup>. In the analysis of the (e,e'f) data the photofission cross sections are necessary to the evaluation of the form factors at the "photon point"<sup>3,4)</sup>. Therefore, the photofission cross sections play a crucial role in the delineation of the GQR fission decay parameters.

Since the advent of monoenergetic photon beams, the photoneutron cross sections have been measured systematically for most of the nuclides throughout the periodic table<sup>5)</sup>. Such investigation has been carried out particularly by the Livermore and Saclay laboratories. As a result from this effort, the parameters of the GDR have been delineated and the neutrons and fission branching ratios have been determined as well. However, by examining the Livermore and Saclay results we notice that the cross sections from these two laboratories present serious discrepancies, especially regarding absolute values. It seems to us that the most alarming discrepancy is found in the photofission cross section  $\sigma_{\gamma,f}$  of  $^{232}\text{Th}$ , because the integrated cross section  $A_{\gamma,f} = \int_0^{18} \sigma_{\gamma,f}(\omega) d\omega$  obtained at Livermore ( $\omega$  is

the excitation energy in MeV) is about 40% bigger than the one obtained at Saclay, while the shapes of the  $\sigma_{\gamma,f} \times \omega$  from these two laboratories are in good agreement.

This fact motivated us to perform a careful measurement of the bremsstrahlung-induced fission cross section for  $^{232}\text{Th}$ . The main characteristics of this experiment, when compared to the photofission one<sup>5-7)</sup>, are:

- (1) the intensity of the bremsstrahlung photon beam propitiates the obtention of fission yields with much better statistics;
- (2) the fission fragments are detected directly using mica foils track detectors avoiding, therefore, the need of fission neutron multiplicity calculation;
- (3) the bremsstrahlung-induced fission  $\sigma_{B,f}$  is sensitive to the photofission area  $A_{\gamma,f}$ , because

$$\sigma_{B,f}(E_e) = \int_0^{E_e} \sigma_{\gamma,f}(\omega) N^B(E_e, \omega) d\omega \quad (1)$$

where  $E_e$  is the electron incident energy, and  $N^B$  is the bremsstrahlung spectrum. As  $N^B$  is to a reasonable approximation proportional to  $\omega^{-1}$  we observe that<sup>2)</sup>  $\sigma_{B,f} \propto B(E1) \cdot P_f$ , where  $B(E1)$  is the reduced transition probability for the GDR, and  $P_f$  is the fission probability. However,  $\omega_R \cdot B(E1) \cdot P_f \propto A_{\gamma,f}$ , in the case of assuming all the GDR strength concentrated in a single isolated level  $\omega_R$  (the resonance peak).

We measured  $\sigma_{B,f}(E_e)$ , for  $E_e$  ranging from 20 to 32 MeV, using the electron beam of the University of São Paulo Linear Accelerator and mica foils as fission detectors at different angles with respect to the incident beam direction.

The absolute mass of the  $^{232}\text{Th}$  target,  $153 \mu\text{g}/\text{cm}^2$  thick, was determined by alpha counting to  $\pm 4\%$ . A copper radiator,  $970 \text{mg}/\text{cm}^2$  thick, was attached behind the target and the set was placed in the center of the reaction chamber making an angle of  $45^\circ$  with the electron beam. The electron beam was monitored by a secondary emission monitor (SEM), before the radiator and the target; the calibration of the SEM was accomplished by using a Faraday cup to  $\pm 3\%$ . Contamination (of the order of 10%) of the photofission yields with electrofission events was accounted for by means of the method developed by Barber<sup>8)</sup>. Also, the data were corrected for the finite thickness of the radiator utilizing the procedures described in Ref. 9. Other details concerning the beam monitoring device, reaction chamber, accelerator, etc., were published elsewhere<sup>2,9)</sup>.

Figure 1 shows the results (data points) of this work for  $\sigma_{B,f}$ ; the error flags contain the propagation of both count-rate statistics ( $\sim 1\%$ ) and systematic uncertainties (in the target thickness, detectors solid angles, and beam monitoring device), and are typically  $\sim 7\%$ . The shaded bands were obtained by numerical integration of the photofission cross sections from Saclay and Livermore in the kernel of eqn. 1, using the bremsstrahlung spectrum calculated in the Davies-Bethe-Maximon approximation<sup>10)</sup> (DBM), which is the most appropriate approach in the energy region here investigated<sup>11)</sup>. The  $\sigma_{\gamma,f}$  were obtained above 18 MeV by extrapolation of the experimental points below 18 MeV, by means of a Lorentz curve up to  $\sim 30$  MeV. However, the integral cross sections  $\sigma_{B,f}(E_e)$  for  $E_e > 18$  MeV are nearly insensitive to small changes in the tail of the GDR till  $\sim 30$  MeV.

In Fig. 2 are shown the ratio of  $\sigma_{B,f}$  measured

in this Laboratory to those generated from the  $\sigma_{\gamma,f}$  of the literature (see Fig. 1). In order to simplify the notation we name these ratios as SP/L and SP/S, standing for São Paulo/Livermore and São Paulo/Saclay, respectively. The mean values are

$$\left\langle \frac{\text{SP}}{\text{L}} \right\rangle = 1.09 \pm 0.05 \quad \text{and} \quad \left\langle \frac{\text{SP}}{\text{S}} \right\rangle = 1.75 \pm 0.08$$

As mentioned before, the discrepancies exhibited by Livermore and Saclay data are not restricted to the  $^{232}\text{Th}$  photofission cross sections. Recently, Wolyneć *et al.*<sup>12)</sup> showed that the differences between the Saclay and Livermore ( $\gamma,n$ ) and ( $\gamma,2n$ ) cross sections arise from the neutron multiplicity sorting, and that preliminary data for  $^{181}\text{Ta}$  indicate that the neutron multiplicity sorting carried out by Livermore is correct.

As illustration, in Fig. 3 is shown how the utilization of the available photofission data affects the interpretation of an electrofission experiment. In this figure the data points are  $^{232}\text{Th}$  electrofission cross sections measured at Giessen<sup>13)</sup>, and the curves were obtained by integrating the photofission cross sections with the E1 virtual-photon spectrum; therefore, they nearly correspond to a pure E1 electrofission process. Using Saclay's results (curve S in Fig. 3) in the data interpretation, we conclude that the  $^{232}\text{Th}$  (e,f) process cannot be explained as proceeding through pure E1 transitions. On the other hand, the Giessen electrofission cross section falls systematically below the Livermore E1-curve (curve L in Fig. 3); therefore, no physical information can be outlined. It is possible to speculate about miscalculation of the E1 virtual-

photon spectrum, as suggested recently<sup>14)</sup>; however, it is worth remembering that the E1 virtual-photon spectrum calculation was tested experimentally again in a recent work carried out at the NBS<sup>11)</sup>. We are performing very detailed measurements of the  $^{232}\text{Th}$  electrofission cross section, in the energy range 5 - 32 MeV, which will be the subject of a forthcoming publication; the preliminary results indicate that the Livermore photofission cross section for  $^{232}\text{Th}$  accounts for the majority of the electrofission process.

#### REFERENCES

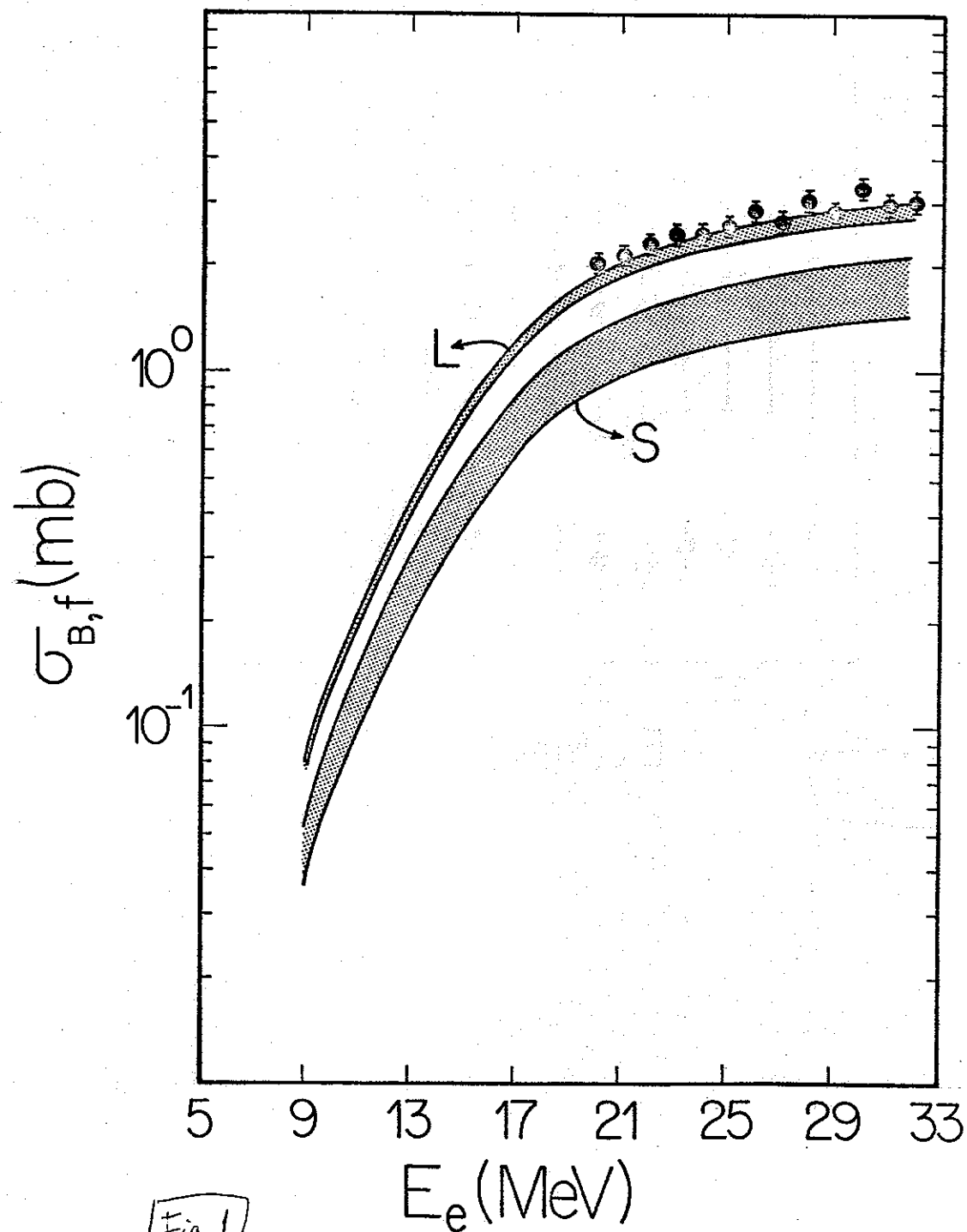
- 1) J.D.T. Arruda-Neto and B.L. Berman, Nucl. Phys. A349, 483 (1980).
- 2) J.D.T. Arruda-Neto et al., Nucl. Phys. A389, 378 (1982).
- 3) J.D.T. Arruda-Neto, "Coincident-Inclusive electrofission angular correlations", J. Phys. G: Nucl. Phys. (in press).
- 4) D.H. Dowell et al., Phys. Rev. Lett. 49, 113 (1982).
- 5) "Atlas of Photoneutron Cross Sections obtained with mono-energetic photons", Lawrence Livermore National Laboratory, Preprint UCRL-78482, ed. B.L. Berman (1976).
- 6) A. Veyssière et al., Nucl. Phys. A199, 45 (1973).
- 7) J.T. Caldwell et al., Phys. Rev. C21, 1215 (1980).
- 8) W.C. Barber, Phys. Rev. 111, 1642 (1958).
- 9) J.D.T. Arruda-Neto et al., Phys. Rev. C22, 1996 (1980).
- 10) H.A. Bethe and L.C. Maximon, Phys. Rev. 93, 768 (1954), and H. Davies et al., Phys. Rev. 93, 788 (1954).
- 11) W.R. Dodge et al., Phys. Rev. C28, 150 (1983), and references herein.
- 12) E. Wolyneć et al., University of São Paulo, Pre-print IFUSP/P-404 (to be published).
- 13) J. Aschenbach et al., Z. Phys. A292, 285 (1979).
- 14) H. Ströher et al., Phys. Rev. Lett. 47, 318 (1981).

FIGURE CAPTIONS

Fig. 1 - Data points: bremsstrahlung-induced fission cross sections for  $^{232}\text{Th}$ . Shaded bands: photofission cross sections from Saclay (S) and Livermore (L) integrated in the bremsstrahlung spectrum (details in the text); the width of the bands represents the experimental uncertainties associated with the photofission cross sections.

Fig. 2 - Ratio of the bremsstrahlung-induced fission cross sections, from the present work (SP), to those generated from the Saclay (S) and Livermore (L) photofission cross sections.

Fig. 3 - Data points: electrofission cross section of  $^{232}\text{Th}^{13}$ . Curves: photofission cross sections from Saclay (S) and Livermore (L) integrated in the E1 virtual-photon spectrum.



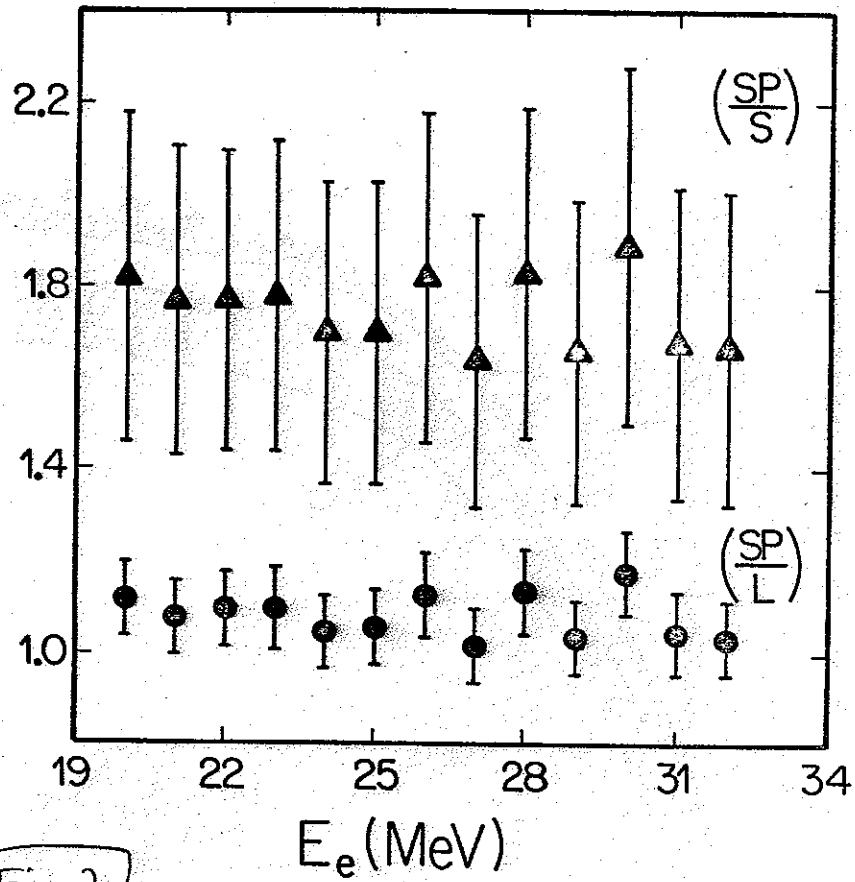


Fig. 2

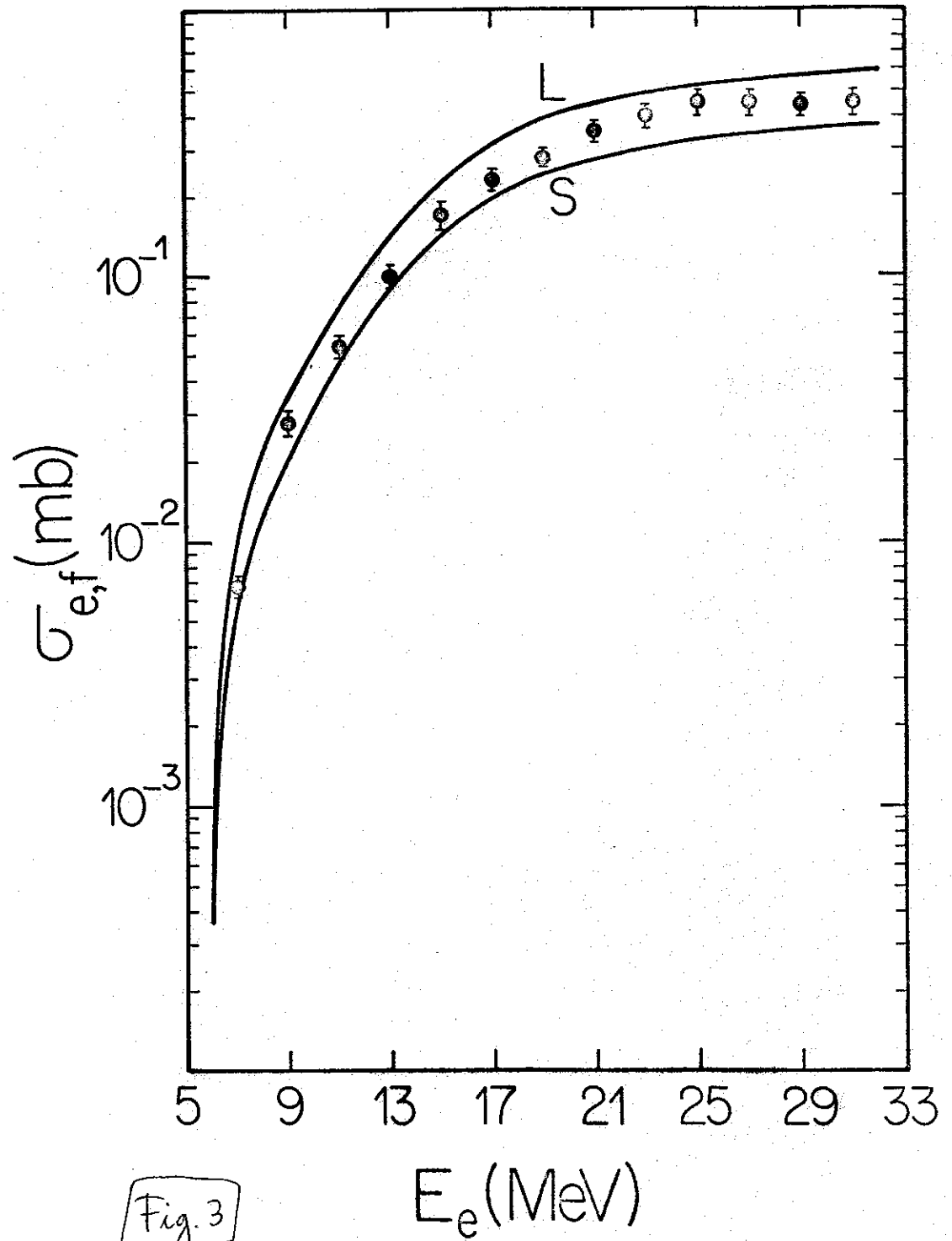


Fig. 3